Developmental Biology 349 (2011) 169–178

Contents lists available at ScienceDirect

Developmental Biology

journal homepage: www.elsevier.com/developmentalbiology

A novel function for KIF13B in germ cell migration

Katsiaryna Tarbashevich [1], Aliaksandr Dzementsei, Tomas Pieler *

Dept. Developmental Biochemistry, GZMB, 37077 Goettingen, Germany

ARTICLE INFO

Article history:
Received for publication 28 February 2010
Revised 19 September 2010
Accepted 14 October 2010
Available online 26 October 2010

Keywords:
Xenopus
Primordial germ cells
KIF13B
PIP3

ABSTRACT

Primordial germ cell (PGC) development in *Xenopus* embryos relies on localised maternal determinants. We report on the identification and functional characterisation of such one novel activity, a germ plasm associated mRNA encoding for the *Xenopus* version of a kinesin termed *KIF13B*. Modulations of xKIF13B function result in germ cell mismigration and in reduced numbers of such cells. PGCs explanted from *Xenopus* embryos form bleb-like protrusions enriched in PIP3. Knockdown of xKIF13B results in inhibition of blebbing and PIP3 accumulation. Interference with PIP3 synthesis leads to PGC mismigration in vivo and in vitro. We propose that xKIF13B function is linked to polarized accumulation of PIP3 and directional migration of the PGCs in *Xenopus* embryos.

Introduction

Primordial germ cells (PGCs) in *Xenopus* embryos inherit maternal determinants that localize to the vegetal pole of the oocyte. This material includes a number of different vegetally localizing mRNAs, encoding for the RNA binding proteins *Germes* and *XDead end* (Berekelya et al., 2003; Horvay et al., 2006), for the translational regulators *Xcat2* and *Xdazl* (Houston et al., 1998; MacArthur et al., 1999), as well as for the scaffolding protein *XGRIP2* (Kirilenko et al., 2008; Tarbashevich et al., 2007) and for *Xpat*, a major component of the germ plasm proposed to function in its structural organisation (Hudson and Woodland, 1998). Translational inhibition of such proteins has either resulted in a loss of PGC specification/differentiation, or in disturbed PGC migration (Houston and King, 2000a; Kirilenko et al., 2008; Tarbashevich et al., 2007).

During development, *Xenopus* PGCs first migrate passively with the gastrulation movements of the embryo and later, during tailbud and tadpole stages, actively, first laterally/anteriorly and then dorsally/anteriorly (Heasman and Wylie, 1981; Houston and King, 2000a; Tarbashevich et al., 2007; Whitington and Dixon, 1975). *Xdazl* was reported to be required for proper dorsal migration (Houston and King, 2000a), while *XGRIP2* was found to be involved in the initial anterior migration of the PGCs (Tarbashevich et al., 2007). Much of the molecular mechanisms that underlie these directional cell movements remain to be worked out. While pioneering studies had revealed that fibronectin can serve as a substratum for PGC migration (Heasman et al., 1981), the molecular basis of motility remains to be defined in the *Xenopus* system.

Significant advances concerning the chemotactic nature of PGC migration have been made more recently in the zebrafish (Boldajipour and Raz, 2007). In particular, a signalling system that guides PGC migration has been identified; the chemokine SDF-1a serves as a signal operating via the G-protein coupled receptor CXCR4b that is expressed in the PGCs. CXCR4 knockdown results in non-directional PGC migration, while an ectopic source of SDF-1a is sufficient to attract the PGCs in the fish (Doitsidou et al., 2002). A second SDF-1a receptor, CXCR7, which is mainly expressed in the somatic tissue, has been proposed to fine-tune SDF-1a gradient formation by clearing the excess of the ligand (Boldajipour et al., 2008). Directional migration of zebrafish PGCs has been found to depend on the function of the Gi subunit in G-protein-coupled receptors (Dumstrei et al., 2004). The SDF-1/CXCR4-system may equally operate in directing PGC migration in other organisms, such as mouse, chicken, Medaka and perhaps also in *Xenopus* (Ara et al., 2003; Herpin et al., 2007; Molyneaux et al., 2003; Stebler et al., 2004; Takeuchi et al., 2010). In the mouse, chemoattractant activity on PGC migration has also been reported for the Kit ligand (KL); KL may operate via PI3 kinase as its downstream effector in this context (Farini et al., 2007).

Cellular mechanisms governing cell polarization and directional PGC migration in response to chemotactic cues have been analyzed in the zebrafish; PGCs form bleb-like protrusions coinciding with sites of elevated free calcium (Blaser et al., 2006). Formation of spherical membrane protrusions, referred to as blebs, has been associated with cell movement in various biological systems, including tumor cells migrating through the extracellular matrix (Charras and Paluch, 2008). Blebbing is initiated as a local dissociation of the plasma membrane from the cortex, followed by pressure-driven bleb expansion. Reformation of an actomyosin cortex is followed by bleb retraction. How polarized bleb formation is initiated and functions as a basis for directional cell migration remains to be worked out in

* Corresponding author. Fax: +49 551 3914614.
E-mail address: tpieler@gwdg.de (T. Pieler).
[1] Present address: Institute of Cell Biology, ZMBE, 48149 Muenster, Germany.

0012-1606/$ – see front matter © 2010 Elsevier Inc. All rights reserved.
doi:10.1016/j.ydbio.2010.10.016

detail. In several systems, including *Dictyostelium discoideum*, PIP3 enrichment in blebs was found to be associated with exposure to chemoattractants (Kortholt et al., 2007; van Haastert et al., 2007); however, a more recent systematic mutational study in *Dictyostelium* has revealed chemotaxis in the absence of PIP3 gradients, albeit defects in movement speed were observed (Hoeller and Kay, 2007). It therefore seems that multiple, intertwined signalling pathways operate intracellularly in response to a chemoattractant, at least one of which involving PIP3 (King and Insall, 2008).

Here, we describe polarized bleb formation with enrichment of PIP3 as an important element for the directional PGC migration in *Xenopus* embryos. A novel activity functioning in this context is kinesin 13B (xKIF13B); it is encoded by a vegetally localizing oocyte mRNA that is found to be associated with the germ plasm. Its activity is required for the formation of polarized blebs in explanted *Xenopus* PGCs, as well as for proper PGC migration in *Xenopus* embryos and in vitro.

Materials and methods

Cloning procedures

xKIF13B 5′UTR_ORF_DE contains the 5′UTR and the ORF of *xKIF13B*. *xKIF13B ORF_DE* represents the ORF of *xKIF13B*. *DsRED_xKIF13B ORF_DE* consists of the *DsRED* ORF fused in frame with the *xKIF13B* ORF. *EGFP_GRPIPH_DE* contains the *EGFP* ORF fused in frame to the PH domain of the *GRPI* protein (Dumstrei et al., 2004; Klarlund et al., 1997). *xPTEN_DE* and *dnPI3K_DE* represent, correspondingly, the ORF of *xPTEN* and the dominant-negative *PI3K* version (Dumstrei et al., 2004; Hara et al., 1994). All the constructs described earlier were tagged by the *xDead End* (Horvay et al., 2006) 3′UTR. Injection of mRNAs produced from these plasmids results in PGC specific stabilization of the transcript (Koebernick et al., 2010; Tarbashevich et al., 2007).

xKIF13B 5′UTRmycGFP contains the 5′UTR of *xKIF13B* upstream of the *mycGFP* ORF (Klisch et al., 2006). *xKIF13B_ MD*, *xKIF13B MD_2490* and *xKIF13B MD_3438* represent fragments of the *xKIF13B* ORF containing the full motor domain only or together with a part of the stalk domain (ending with the nt 2490 and nt 3438, respectively).

The full-length 5845 bp cDNA of *xKIF13B* (Gen Bank ID EU930364) was obtained by extensive 5′/3′RACEing of the initial 800 bp ORF fragment. *xPTEN* ORF was obtained by PCR from the total embryonic cDNA (for sequences of primers see Table S4).

Preparation of sense mRNAs, antisense riboprobes, and whole mount in situ hybridization

Whole mount in situ hybridization (WMISH) was performed with *Xenopus laevis* embryos as described previously (Hollemann et al., 1999). Antisense riboprobes were produced by standard in vitro transcription from linearized plasmids in the presence of digoxygenin-coupled rUTP. *MyoD* and *Xpat* antisense RNA probes were generated as described by Tarbashevich et al. (2007). The *xKIF13B* antisense RNA probe was generated from four plasmids: *xKIF13B MD* pGEM-T easy, *xKIF13B MD_2490* pGEM-T easy, *xKIF13B MD_3438* pGEM-T easy, and *xKIF13B ORF* pGEM-T easy. *xKIF13B MD_2490* pGEM-T easy, *xKIF13B MD_3438* pGEM-T easy, and *xKIF13B ORF* pGEM-T easy were linearized by *SpeI* followed by T7 RNA polymerase mediated in vitro transcription. *xKIF13B MD* pGEM-T easy was linearized with *SacII* followed by Sp6 RNA polymerase mediated in vitro transcription. Images of stained embryos were taken directly after the colour reaction under the Olympus DF PLAPO 1.2× PRZ microscope.

Sense mRNAs were in vitro transcribed from *NotI* linearized plasmids using the MESSAGE mMASCHINE kit (Ambion) and purified by Illustra™ RNA spin MiniRNA Isolation Kit (GE Healthcare) according to manufacturers' protocol.

Manipulations of Xenopus laevis embryos

Embryos were obtained from *X. laevis* females by human chorionic gonadotropin (HCG) (Sigma) induced egg-laying (800–1000 U HCG injected approximately 12 h before egg-laying). Spawns were in vitro fertilized with minced testis in 0.1× MBSH, dejellied with 1.5–2% cystein hydrochloride (pH 7.8) and cultured in 0.1× MBSH at 14 °C. Albino embryos were stained with Nile Blue (0.01% (w/v) Nile Blue chloride, 89.6 mM Na_2HPO_4, 10.4 mM NaH_2PO_4, pH ~7.8) for 10 min at RT prior to injections to distinguish between animal and vegetal poles. Injections were performed in injection buffer (1% (w/v) FICOLL in 1× MBS) on a cold plate (12.5 °C) vegetally into both blastomeres of two-cell stage embryos. 1–4 nl of mRNA and/ or morpholino oligonucleotide solutions was injected per blastomere. Embryos were kept for at least 1 h in the injection buffer at 12.5 °C before transfer into 0.1× MBSH.

Analysis of PGC migration

The migration phenotype was scored by two parameters: a) by calculating the area occupied by migrating germ cells ("spreading") and b) by counting the number of PGCs detected outside of their normal A/P position ("mislocalization"). Mislocalization of PGCs along the A/P axis was calculated as described by Tarbashevich et al. (2007). In brief, experimental embryos were fixed at stage 32–33 and stained for *Xpat*/*MyoD* by WMISH. PGC positioning in between somites 5 and 11 was scored as normal; PGCs outside of this region were scored as mislocalized (see also Figs. 2C–F). Average numbers were calculated in respect to the total PGC number scored for the given experiment (in groups of 20 embryos for each kind of treatment). Final results were averaged from three independent injection series. PGC "spreading" was calculated as the surface area of PGC distribution (the area of an ellipse containing all PGCs on the given side of an embryo). To take into account differences in the size of the embryos, this value was normalized against the area of a square with the diagonal equal to the distance between the first two somites of a given embryo. Average numbers were calculated for groups of 20 embryos for each kind of treatment. Final results were averaged from three independent experiments. Statistical significance was verified by the paired one-tailed *T*-test.

Culturing of isolated PGCs

Embryos were co-injected at the 2-cell stage with 50 pg of the synthetic mRNA encoding for farnesylated *RFP* ORF (mRFP) together with 0.2 ng of the *EGFP_GRPIPH_DE* mRNA and dissected at stage 30–31 into dorsal and ventral parts (Fig. 5A). Ventral explants were placed in a 30 mm Petri-dish coated with 0.7% agarose, disaggregated in the accutase solution (Sigma), washed with 0.8× MBSH and Danilchik's for Amy (DFA)-medium (53 mM NaCl, 5 mM Na_2CO_3, 4.5 mM potassium gluconate, 32 mM sodium gluconate, 1 mM $MgSO_4$, 1 mM $CaCl_2$, and 0.1% (w/v) BSA, pH 8.3 with 1 M bicine, filtered and stored at −20 °C) and transferred onto a fibronectin-coated Petri-dish. For chemical inhibition of the PI3K signalling, cells were incubated with 100 μM LY294002 (LC Laboratories) in the DFA-medium. The overall behaviour of PGCs was monitored by time-lapse imaging using a LumarV.12 fluorescence stereomicroscope (Zeiss) (GFPA and RFP filter), and the AxioPlan software (Zeiss). Time-lapse movies were acquired at RT for 5 min with 1 frame per 10 s image collection mode.

PGC polarity assay

One half of a 30 mm Petri-dish was filled with 0.5% agarose. After agarose polymerization, the other half of the dish was coated with fibronectin (Sigma) according to the manufacture's protocol. Tailbud stage embryos were dissected to obtain ventral and dorsal explants (see also Fig. 5A). Crude protein extracts were prepared from both types of explants by homogenization and pipetting on ice in the presence of

0.2 mM PMSF to prevent protein degradation. Isolated PGCs (prepared as described earlier) were transferred into DFA-medium and placed onto the fibronectin-coated half of a Petri-dish with the DFA-medium. The medium was in contact with the vertical part of the agarose sector only, avoiding it's spreading onto the horizontal agarose surface. 5 μl of the corresponding crude protein extract each was injected into opposite corners of the agarose sector of a Petri-dish by use of a syringe only after the dish was positioned on the microscope mount in order to minimise disturbance of the medium. Membrane dynamics and migration of isolated PGCs was observed by time-lapse microscopy using a LumarV.12 fluorescence stereomicroscope (GFPA and RFP filter) and the AxioPlan software (Zeiss). Time-lapse movies were acquired at RT for 5 min with 1 frame per 10 s image, or for 100 min with 1 frame per 1 min image collection. Directionality of protrusion formation for each PGC in the field was documented at each frame in respect to the extract gradient (a protrusion sent towards the extract was regarded as formed "Up" the gradient). The average number of protrusions sent by PGCs into a certain direction was calculated as percentage over the total number of protrusions documented in a given experiment. Results were averaged between three independent experiments and represented in form of a radar-graph.

Antibodies

Primary antibodies: αKIF13B (Abnova, diluted 1:100), αGAPDH (Santa Cruz, diluted 1:5000), αActin (Sigma, 1:5000), and αMyc (Sigma, diluted 1:5000). Secondary antibodies: goat-anti-mouse HRP-coupled (Sigma, diluted 1:20,000), and goat-anti-rabbit HRP-coupled (Sigma, diluted 1:10,000). The ECL Direct™ labeling and detection system (Amersham) was used to visualize proteins.

Results

An N3-family kinesin is encoded by a vegetally localizing mRNA associated with the Xenopus germ plasm

A microarray-based screen was performed in order to identify novel, vegetally localizing mRNAs in *Xenopus* oocytes (Horvay et al., 2006). The ORF for one of these encodes for a ~250 kDa protein most closely related to the mammalian kinesin 13B (Fig. S1) and was therefore named xKIF13B for *Xenopus* kinesin 13B. Kinesin 13B belongs to the KIF-N3 family of plus-end motor proteins responsible for the directional transport of synaptic and receptor-cargo vesicles to the cell membrane (Hirokawa and Takemura, 2005; Miki et al., 2001). Structurally, KIF13B-proteins consist of a conserved motor domain, a cargo-binding stalk domain, as well as of the C-terminal Cap-Gly domain, also referred to as the cytoskeleton-associated glycine-rich domain, involved in interactions with microtubules and intermediate filaments. For the *Drosophila* and mammalian homologues of *KIF13B*, two main cargo molecules were identified: the membrane-associated guanylate kinase homologue scaffolding protein hDlg/SAP97, and centaurin-α1, a PIP3-binding protein; both proteins were implicated in the establishment of cell polarity and in cell adhesion (Asaba et al., 2003; Venkateswarlu et al., 2005).

During earliest stages of *Xenopus* oogenesis, *xKIF13B* mRNA is translocated to the tip of the vegetal cortex that harbours the germ plasm (Figs. 1A and B); *xKIF13B* mRNA remains associated with this material during early embryogenesis and persists in the PGCs at tailbud stage (Figs. 1C,D and G); in addition, zygotic expression is detected in the central nervous system and in the migrating neural crest cells (Figs. 1E–G, Fig. S2).

Modulation of xKIF13B activity affects PGC migration in Xenopus embryos

Spatio-temporal expression characteristics of *xKIF13B* suggest a possible involvement in the specification and/or migration of *Xenopus* PGCs. To address this question, overexpression and antisense morpholino oligonucleotide (MO) mediated knockdown experiments were performed; activity and specificity of the two different MOs employed were verified *in vitro* and *in vivo* (Fig. S3). Microinjection of either of these MOs resulted in a decrease of the average number of PGCs, as well as in PGC migration defects during tailbud stages of development (Fig. 2, Fig. S5, Table S1). In control embryos, PGCs are generally found to migrate as a compact group of cells, while in the xKIF13B morphant embryos, they are reduced in number and found to be spread out over a 2–3 fold larger area, expanding both along the anterior–posterior and the dorsal–ventral body axes. Both phenotypic effects, on average PGC number as well as on PGC migration, were partially rescued by co-injection of *xKIF13B ORF_DE* at a low concentration (Fig. 2G, Table S1). Microinjection of high concentrations of *xKIF13B ORF_DE* mRNA equally results in approximately 2-fold reduced average numbers and disturbed migration of PGCs (Fig. 2G, Table S1). The migratory defects observed suggest that xKIF13B might be involved in the establishment of PGC polarity, which is in line with functional data from other cell systems (Asaba et al., 2003; Venkateswarlu et al., 2005). Similarities of gain- and loss-of-function phenotypes suggest that the normal functioning of xKIF13B is dose-dependent.

Modulation of xKIF13B activity affects PGC morphology, dynamics of protrusion formation and PIP3 distribution

It was previously postulated that KIF13B might be involved in the regulation of neuronal polarity by trafficking of PIP3-vesicles to the tips of growing neurites (Horiguchi et al., 2006); these ideas prompted us to test for a possible correlation between the activity of xKIF13B on the one hand and PIP3 distribution within *Xenopus* PGCs on the other. In order to visualize the intracellular localization of PIP3, we made use of a GFP-GRPI-PH domain fusion construct specifically binding to PIP3 (Dumstrei et al., 2004; Klarlund et al., 1997); the 3′-UTR of the corresponding construct contains the *XDead end* localization element, restricting protein expression to the PGCs (Horvay et al., 2006; Koebernick et al., 2010). Intracellular localization of PIP3 in the PGCs of intact embryos is detectable by confocal and two-photon microscopy. PIP3 is found to be enriched at the membrane and in the peri-membranous space at the leading edge of the PGCs (Fig. 3A). Time-lapse analysis of PIP3 distribution was performed with dissociated PGCs from endodermal explants, cultured on fibronectin (see Materials and methods for details). Under these conditions, PGCs form dynamic, transient protrusions (blebs), which are strongly enriched in PIP3 (Figs. 3B,B″, and C, Movie S1, Table S2). In more than half of the PGCs isolated from xKIF13B morphant embryos, formation of such protrusions was no longer detected (Fig. 3D, Table S2), while some of these PGCs formed unusual filopodia-like membrane extensions with seemingly decreased concentrations of PIP3 (Fig. 3E, Table S2). Overexpression of *xKIF13B*, which also results in migratory defects (see earlier discussion), leads to an elevation of the PIP3 signal intensity throughout the PGC plasma membrane, and number as well as size of protrusions forming in such cells were found to be irregular (Fig. 3F). Analysis of the subcellular distribution of a tagged version of xKIF13B reveals its enrichment at the bleb membrane (Fig. 3G). Taken together, these findings provide strong indications for xKIF13B function being linked to PIP3 accumulation at the site of membrane blebbing.

Inhibition of the PI3K-signalling affects PGC migration and number, as well as the dynamics of blebbing

The experiments described earlier suggest a functional link between PGC migration and PIP3 signalling. In order to test this possibility more directly, we modulated PIP3 signalling in PGCs by overexpression of either a dominant-negative version of the PI3 kinase (dnPI3K) (Dumstrei et al., 2004; Hara et al., 1994), or of *Xenopus* PTEN (xPTEN),

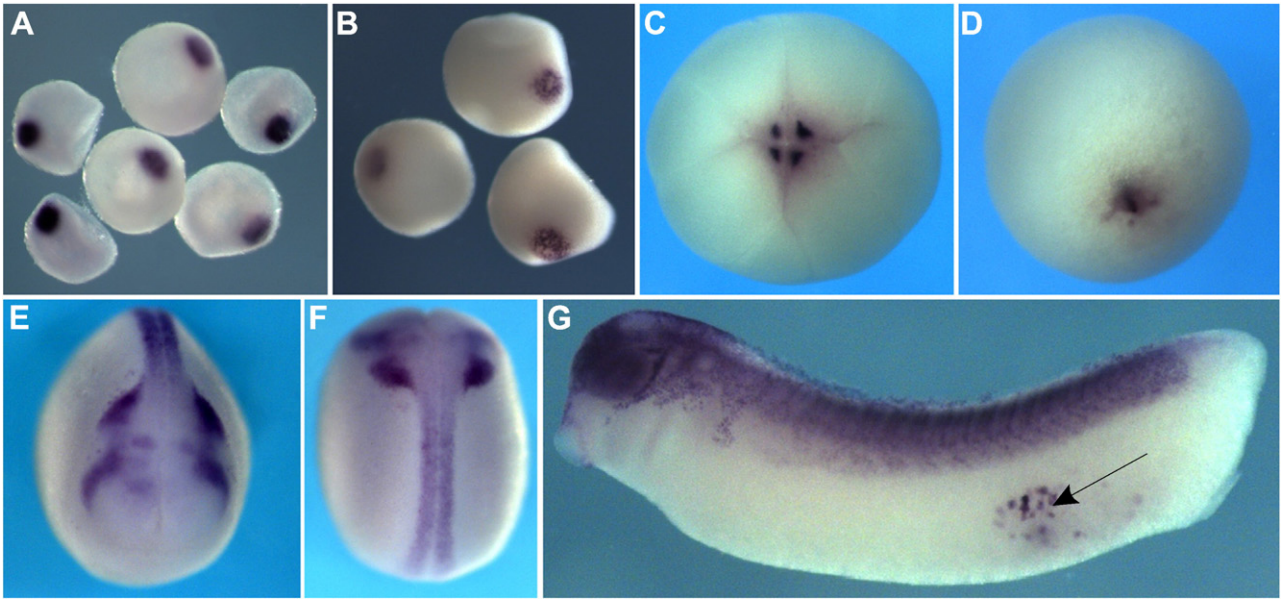

Fig. 1. *xKIFI3B* expression characteristics during oogenesis and embryogenesis. (A–G) *xKIF13B* mRNA was detected by whole mount in situ hybridization. During oogenesis, *xKIF138* mRNA localizes to the tip of the vegetal cortex; A. early (stage II) oocytes; and B, late (stage III–IV) oocytes. At the 4-cell stage, *xKIFI3B* mRNA is enriched in the granular germ plasm islands at the vegetal pole (C, vegetal pole view). At gastrula stage, the transcript is detected in the region of the primordial germ cells (D, blastoporus view). During neurulation, *xKIF13B* mRNA starts to be expressed in the neural tube and in the cranial neural crest cells (E, anterior view, and F, dorsal view). At tailbud stage, *xKIFI3B mRNA* is expressed in PGCs (arrow), neural crest cells, brain, spinal cord and notochord (G, lateral view of the embryo with the head to the left).

mediating degradation of PIP3 (Waite and Eng, 2002); as discussed earlier, both constructs were fused to the *XDead end* 3′-UTR in order to achieve germ cell specific expression. Inhibition of PI3K signalling by these means in the context of whole embryos resulted in increased PGC mismigration and reduced average PGC numbers (Fig. 4; Table S3). Application of low doses of either *xKIF13B* MO1/2 or *xPTEN_DE* alone had no clear effect on PGC number or migration, while co-injection of both resulted in significantly decreased PGC numbers and enhanced PGC mismigration (Fig. 4F). Such a synergism affecting PIP3 enrichment at the membrane in PGCs (decreased PIP3 level by xPTEN overexpression and its impaired localization by xKIF13B knockdown) provides further support for the notion of a functional link between xKIF13B function and PIP3 signalling. Chemical inhibition of PI3K in isolated germ cells by application of LY294002 (van Haastert et al., 2007) had two main effects; 25–30 min after incubation with LY294002, the ability of protrusion formation was lost in about half of the PGCs, while a major portion of cells formed unusual membrane extensions and became paralyzed in this state (Fig. 4D, Table S2). Time-lapse analysis of isolated PGCs revealed impaired dynamics of blebbing upon PI3K inhibition; size and number of protrusions formed were also found to be reduced (Figs. 4A–D). In summary, inhibition of PIP3 signalling exerts similar effects on PGC blebbing and migration as the knockdown of xKIF13B, suggesting a direct functional link.

Embryonic extracts can attract Xenopus PGCs cultured in vitro and induce formation of polarized protrusions

Xenopus PGCs gained from dissociated endodermal explants were cultured on fibronectin in gluconate-enriched DFA-medium (see Materials and methods). In order to test for the existence of chemoattractant signals that would direct PGC migration, they were exposed to a gradient of total dorsal (DEx) or ventral (VEx) embryonic extracts (Figs. 5A and B). Such extracts were applied at two separate spots in the agarose gel at a distance to the PGCs, in order to allow molecules to diffuse into the incubation medium. Migration and cellular dynamics of the PGCs were analyzed by time-lapse imaging. After 10–15 min of application, PGCs started to form polarized bleb-like protrusions, preferentially in the direction of the DEx-gradient (Fig. 5D, Fig. S4); in the absence of DEx, PGCs formed non-directional protrusions (Fig. 5C). Application of the same assay to PGCs isolated from *xKIF13B ORF_DE*, *dnPI3K_DE* or *xPTEN_DE* injected embryos, as well as from xKIF13B morphant embryos, revealed a more random orientation of protrusions forming in the presence of the DEx-gradient (Fig. 5E, and data not shown). PGC polarization in xKIF13B morphants was rescued by co-injection of the *xKIF13B ORF_DE* (Fig. 5F). Directional migration of PGCs towards the putative chemoattractant source was observed occasionally after 75 to 90 min of incubation (Fig. S4, Movie S2). From more than 100 cells analyzed migration towards DEx source was observed in 11 cases; migration against the DEx source did not occur.

Discussion

Experimental observations reported in this communication reveal a function for the maternal kinesin KIF13B in the context of germ cell polarity and migration in *Xenopus* embryos. Explanted PGCs form bleb-like protrusions enriched in PIP3 and the impaired function of xKIF13B affects both, PIP3 enrichment and blebbing. In the embryo, manipulations of xKIF13B activity result in PGC mismigration as well as in reduced numbers of such cells. Direct inhibition of PIP3 signalling has similar effects on PGC number and migration.

PGC migration in Xenopus embryos: cell shape and motility

Active migration of *Xenopus* PGCs is thought to be responsible for: i) the lateral–anterior–dorsal translocation of these cells, as observed during tailbud stages, and ii) for their passage to the site of formation of the future gonads at tadpole stages, first through the dorsal mesentery and then laterally across the dorsal abdominal wall (Heasman and Wylie, 1981). Early quantitative and ultrastructural studies on PGCs during *Xenopus* embryogenesis had reinforced the idea that components of the germ plasm might be involved in regulating directional migration (Kerr and Dixon, 1974; Whitington and Dixon, 1975). Kamimura et al. (1980) had observed that, during the migration phase (stage 33/34), PGCs are polarised and form multiple contact sites with the surrounding endodermal cells through

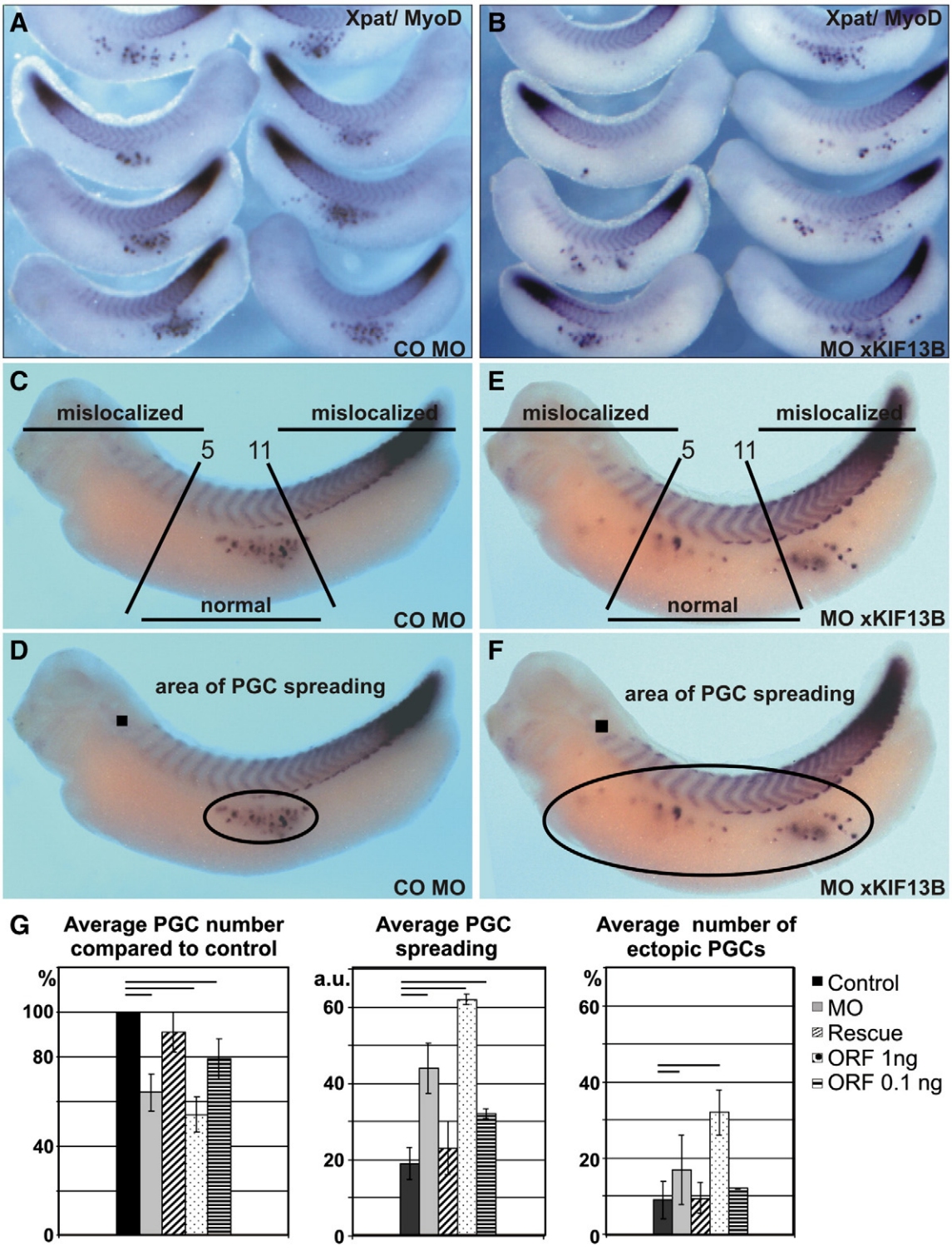

Fig. 2. Knockdown of xKIF13B results in PGC mislocalization. All embryos were stained for *Xpat* (PGC marker) and *MyoD* (somite marker). (A and B) Representative examples of embryos injected with 33.6 ng of control MO (A), or with 16.8 ng of *xKIF13B* M02 (B). Quantifications of the average number of mislocalized PGCs (C and E) and of PGC "spreading" (D and F) in control MO (C and D) and *xKIF13B* MO injected (E and F) embryos (see also Material and methods). (G) *xKIF13B* loss- and gain-of-function reduces the average PGC number and leads to PGC mislocalization. Control embryos were injected with 33.6 ng of control MO: xKIF13B morphants were injected with 16.8 ng of xKIF13B MO2; rescue was performed by co-injection of 16.8 ng of xKIF13B MO2 and 0.1 ng of the *xKIF13B ORF_DE* mRNA; for xKIF13B overexpression 0.1 or 1 ng of the *xKIF13B ORF_DE* mRNA per embryo was injected. For each independent injection 20 embryos per treatment were analyzed. Average PGC numbers were calculated in percentage relative to the control embryos set to 100% for each independent round of injections. PGC spreading represents the minimal ellipse covering the germ cells, normalized to the size of the embryo and represented in arbitrary units (a.u). PGC mislocalization was calculated as percentage of mislocalized (ectopic) PGCs relative to the total PGC number. PGCs were regarded as "mislocalized" when positioned beyond somites 5–11 along the A/P axis of an embryo. Results were averaged between at least three independent rounds of injections. Error bars represent the standard deviation of the mean, lines depict $p<0.05$.

an enlarged intercellular space. This situation is compatible with our proposal of blebbing as the basis for PGC migration, since it could rely on the formation of adhesions with the substratum used for directional movement (reviewed in Charras and Paluch, 2008). However, descriptive studies on PGCs from stage 42/43 embryos, performed both in vivo and in vitro (Heasman and Wylie, 1978), have led to the conclusion that these late migration events occur on the basis of filopodia formation, as well as on waves of contraction and

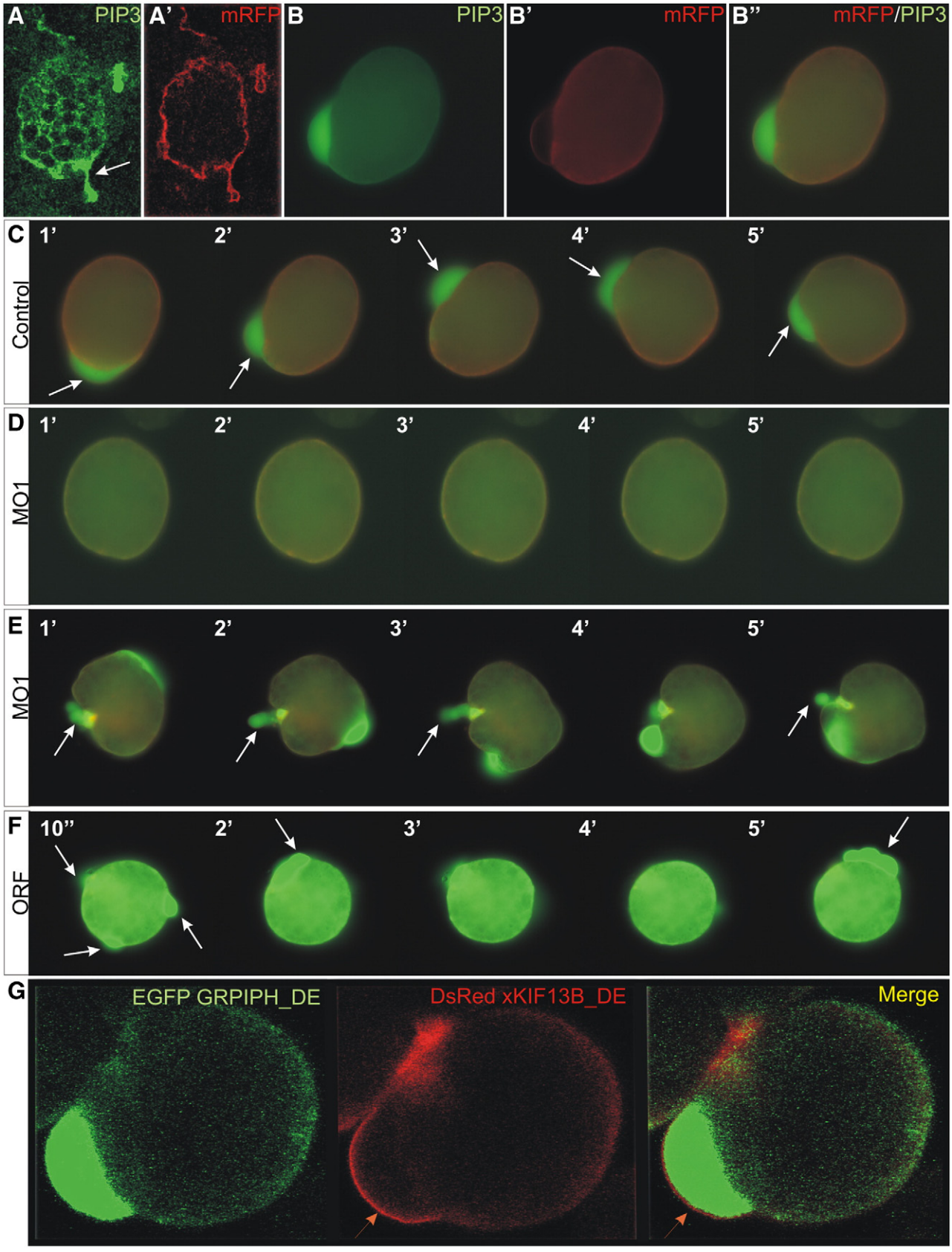

retraction of the trailing edge of these cells. Experiments reported in this communication were with PGCs isolated from early migration phase embryos (stage 30/31) and they provide evidence for amoeboid cell movements, indicating that early and late PGC migration might be subject to distinct mechanisms. Interestingly, in the zebrafish, blebbing has also been reported to constitute the basis for PGC migration in vivo (Blaser et al., 2006).

PGC migation in Xenopus embryos: the maternal contribution

A subpopulation of vegetally localizing mRNAs from *Xenopus* oocytes is associated with the germ plasm; *xKIF13B* represents a novel member of this mRNA family. Similar to the loss-of-function situation described here for *xKIF13B*, MO-mediated knockdown of another vegetally localizing mRNA, *Xdazl*, encoding for an RNA binding protein, was found to affect PGC number and migration (Houston and King, 2000b). The Xdazl protein was subsequently shown to function as a positive translational regulator via direct recruitment of the poly(A) binding protein on Xdazl target mRNAs (Collier et al., 2005). It remains to be determined if *xKIF13B* mRNA could be one of the Xdazl targets, as suggested by the similarity of knockdown phenotypes for these two PGC specific proteins. Inhibition of a different RNA binding protein, *Xenopus* Dead end, whose mRNA is equally associated with the germ plasm, yields loss of PGCs beyond stage 27, when they are found to aggregate, disappearing thereafter (Horvay et al., 2006). In normal *Xenopus* embryos, even though PGCs migrate as a cohort, they are not found to be in direct contact with each other; how this particular feature of their migrational behaviour might be controlled is currently unknown. Yet another vegetally localizing, germ plasm associated mRNA with a function in PGC migration is the one encoding for the glutamate receptor interacting protein *GRIP2* (Kirilenko et al., 2008; Tarbashevich et al., 2007); it is known from experimental systems other than *Xenopus* embryos that GRIP2 and the closely related Grip1 protein function as adapter proteins for different ligands, including transmembrane proteins, and that these proteins play a role in establishing cellular asymmetries (Ataman et al., 2006; Braithwaite et al., 2002; Dong et al., 1997; Schnorrer et al., 2007; Swan et al., 2004). Whether there exists a direct functional link to KIF13B as a transporter molecule remains to be tested.

KIF13B function and PIP3 signalling

It has been suggested that KIF13B functions in the directional transport of PIP3-loaded vesicles in neurites via interaction with a PIP3 binding protein, thereby promoting cellular polarity (Horiguchi et al., 2006). Assuming that xKIF13B serves a similar function in *Xenopus* PGCs, we have tested for PIP3 polarity in such cells and indeed revealed PIP3 enrichment in the blebs forming by PGCs in vitro. Furthermore, xKIF13B knockdown interferes with the intracellular distribution of PIP3. These findings support the hypothesis that xKIF13B-dependent PGC polarity might be involved in the directional migration of these cells. Specific overexpression of *xKIF13B* in PGCs, also observed to interfere with directional migration, could result in elevated ubiquitous levels of PIP3 at the cell membrane and in loss of polarity. Enrichment of PIP2 at the plasma membrane was shown to enhance the membrane-cytoskeleton association, inhibiting membrane blebbing. In contrast, local enrichment of PIP3 by xKIF13B-mediated trafficking or activation of the PI3K, converting PIP2 into PIP3, could destabilize membrane-cytoskeleton interaction and thereby favour protrusion formation (Raucher and Sheetz, 2000; Raucher et al., 2000). In addition to the PIP3 binding protein, KIF13B has also been reported to interact via MAGUK binding site (MBS) with the scaffolding protein hDlg/SAP97, which has a function in cell adhesion (Asaba et al., 2003). Presence of the region homologues to MBS in xKIF13B (Fig. S1) suggests a function of this protein in the regulated formation of PGC–PGC or PGC–somatic cells contacts. Alternatively or in addition to promoting PIP3 polarity, xKIF13B might thus be involved in regulating the formation of cell–cell contacts, an important step in bleb-mediated cell migration.

PIP3 signalling in directional cell migration

Signalling systems directing PGC migration in mouse and zebrafish have been defined. Murine PGCs respond to the Kit ligand in vitro and their migratory activity has been reported to be sensitive towards PI3K inhibitors (Farini et al., 2007). In addition, mice with germ cell specific deletion of the *Pten* gene exhibit enhanced testicular teratomas formation and increased number of ectopic germ cells (Kimura et al., 2003). Together with the observations reported in this communication, these data argue for a conserved function of PIP3 signalling across species in the context of PGC development. Conversely, in the fish system, a distinct signalling system guides PGCs to their destination, namely the chemokine SDF-1a operating through the CXCR4b receptor that is expressed in the PGCs (Doitsidou et al., 2002). CXCR4 was also detected on *Xenopus* PGCs (Nishiumi et al., 2005), and a most recent publication provides some evidence for SDF-1/CXCR4 signalling as being involved in regulating *Xenopus* germ cell migration and survival (Takeuchi et al., 2010). The possibility of zebrafish SDF-1a inducing PI3K activity in the PGCs and thereby regulating their directional migration has been tested experimentally; different from the observations reported here on *Xenopus* PGCs in vitro, polarized distribution of PIP3 in zebrafish PGCs in vivo was not observed. However, the motility of these same cells was found to depend on appropriate levels of PIP3 (Dumstrei et al., 2004). In the same study, it was proposed that PI3K activity might be linked to substrate adhesion, described to be a prerequisite for amoeboid cell movement. Interestingly, PIP3-signalling was found to regulate the directional migration of other cell types, such as *Dictyostelium* amoeba and vertebrate neutrophils (Franca-Koh et al., 2006; Franca-Koh et al., 2007; Yoo et al., 2010); more recent systematic mutational studies in *Dictyostelium* have revealed that multiple parallel pathways are involved in chemotaxis, with each individual one, such as the PI3K pathway, being dispensable (Hoeller and Kay, 2007; King and Insall, 2008; Van Haastert and Veltman, 2007). Multiple pathways might also be involved in regulating the directional migration of *Xenopus*

Fig. 3. Modulation of xKIF13B expression affects morphology, dynamics of protrusion formation and PIP3-mediated polarity in isolated PGCs. (A and B) PIP3 is enriched in the protrusions formed by PGCs (A and A′) confocal microscopy images of a migrating PGC in a living embryo at stage 31. Images were taken in two channels: GFP to visualize *EGFP_GRPIPH_DE* reporter protein as a read-out for the PIP3 signal (A) and RFP to visualize farnesylated RFP (mRFP) labeling the cell membrane (A′). The arrow depicts the PIP3 enrichment in the protrusion at the leading edge of the cell. (B–B″) Fluorescence microscopy images of a PGC isolated from stage 31–32 embryos. Images were taken in two channels: (B) for GFP, to visualize *EGFP_GRPIPH_DE* reporter protein as a read-out for the PIP3 signal, (B′) for RFP to visualize farnesylated RFP (mRFP), labeling the cell membrane. The merged image (B″) reveals enrichment of PIP3 in the protrusion. (C–E) Representative examples for membrane dynamics and PIP3 distribution in cultured PGCs upon modulation of xKIF13B activity. PGCs were isolated from embryos that had been injected with 0.2 ng of the *EGFP_GRPIPH_DE* mRNA alone (C), co-injected with 10 ng of *xKIF13B* MO1 (D and E), or co-injected with 0.5 ng of the *xKIF13B ORF_DE* mRNA (F). Images were selected from time-lapse movies taken for 5 min with a 10 s per frame mode. Arrows indicate PIP3-enriched membrane extensions formed by PGCs. (G) xKIF13B localizes to the membrane of PGC protrusions. 80×-snapshots from the confocal time-lapse movie illustrate the intracellular localization of xKIF13B in an isolated PGC on fibronedin. Cells were isolated form tailbud stage embryos co-injected at two-cell stage with 0.2 ng of the *EGFP_GRPIPH_DE* and 0.3 ng of the *DsRed_xKIF13B ORF_DE* mRNA. Images were taken in two channels: GFP to visualize the PIP3 signal (left image) and RFP for xKIF13B (middle image). The arrow points to xKIF13B enrichment at the membrane of the PGC protrusion.

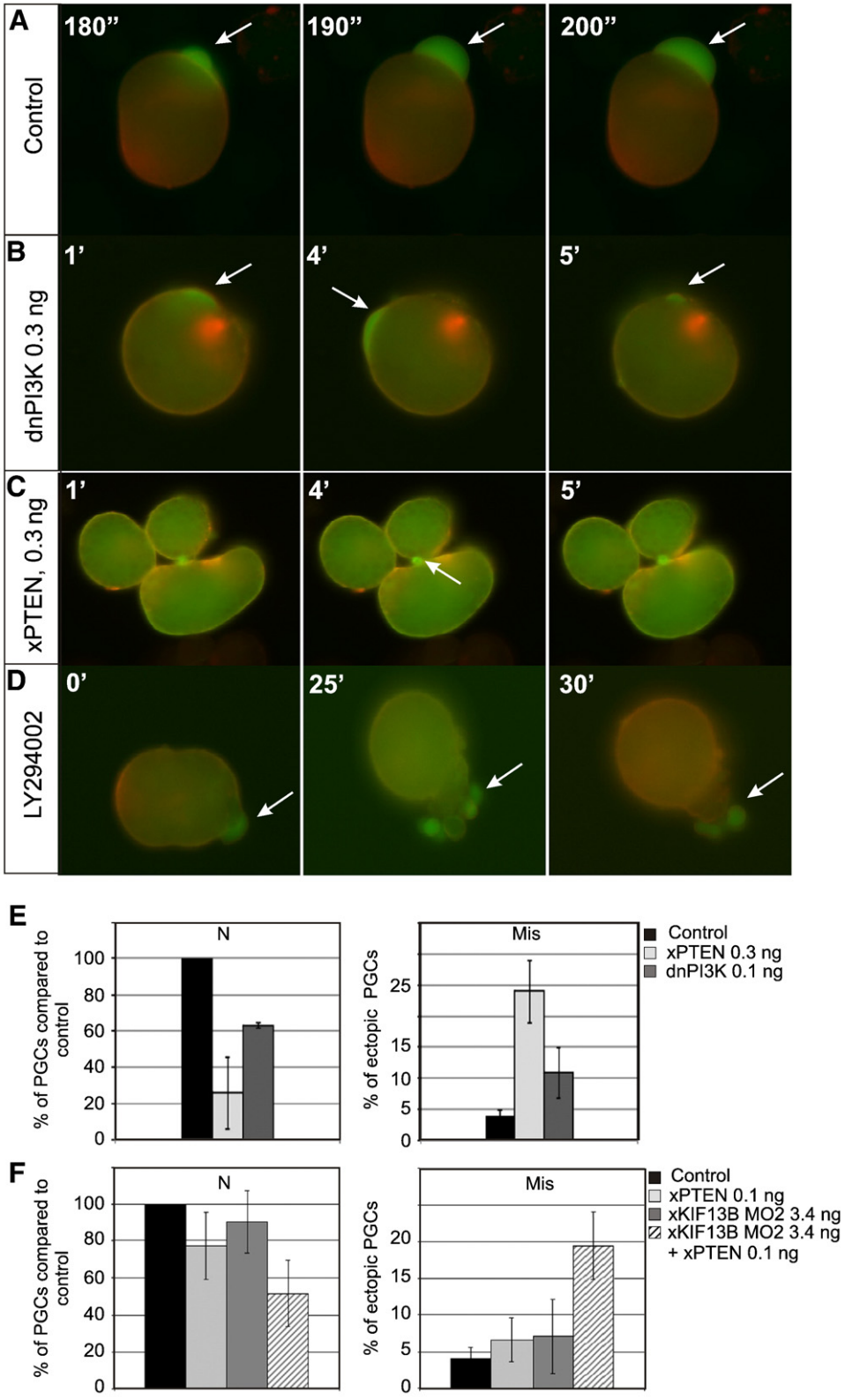

Fig. 4. Inhibition of P13K signalling affects PGC morphology and dynamics of protrusion formation. (A–D) Representative examples of membrane dynamics and PIP3 distribution phenotypes exhibited by cultured PGCs. Cells were isolated from embryos injected with 0.2 ng of *EGFP_GRPIPH_DE* mRNA alone (A),or co-injected with either 0.3 ng of *dnPI3K_DE* mRNA (B), 0.3 ng of *xPTEN_DE* mRNA (C), or incubated in 100 μM LY294002 (D). Images were selected from time-lapse movies acquired for 5 min in the 10 s per frame mode. Arrows indicate PIP3-enriched membrane extensions formed by PGCs. (E–F) Quantification of the phenotypic effects observed upon modulation of xKIF13B activity and PIP3 signalling. Average PGC numbers and mislocalization were calculated as described in the legend to Fig. 2. (E) Overexpression of *xPTEN* or of *dnPI3K* reduces average PGC numbers and leads to increased PGC mislocalization. (F) Synergistic effects of low doses of *xKIF13B* MO and dnPI3K on PGC number and mislocalisation.

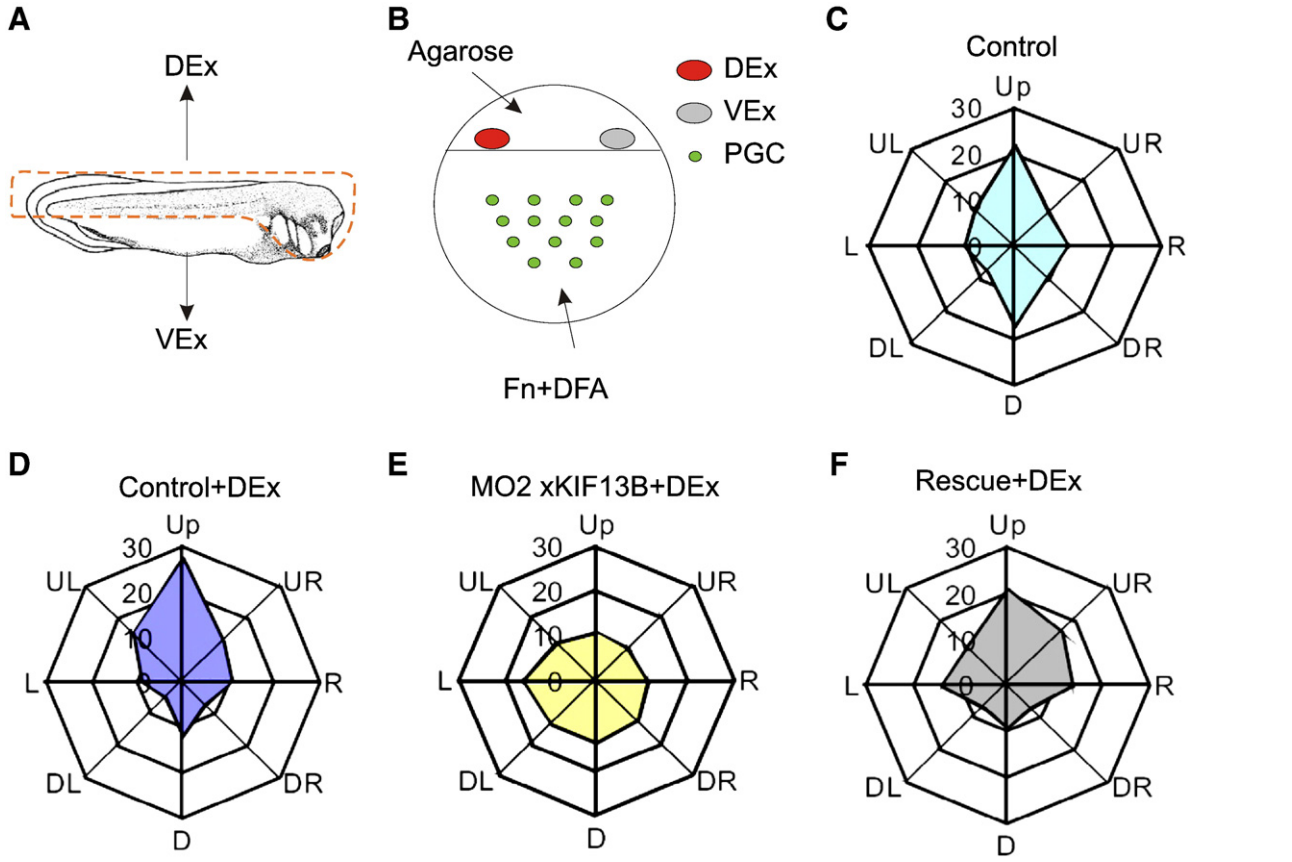

Fig. 5. Protrusion polarity and directional migration *of Xenopus* PGCs in vitro. (A and B) Graphical representation of the PGC polarity assay. (A) Dissection scheme of a tailbud stage embryo. Dorso-anterior parts as indicated by the dotted line were used for the preparation of the dorsal protein extract (DEx), the remaining portion of the embryo was used either for the PGC isolation or for the preparation of the ventral protein extract (VEx). (B) Schematic illustration of the final set up for the PGC polarity assay (see Materials and methods for details). (C–F) Radar-graphs illustrating directionality of protrusion formation by PGCs cultured in the absence (C) or presence (D–F) of DEx. Cells were isolated from stage 30–31 embryos injected with 0.2 ng of *EGFP_GRPIPH_DE* mRNA alone (C and D), or co-injected with 16.8 ng of *xKIF13B* MO2 (E), or co-injected with 16.8 ng of *xKIF13B* MO2 together with 0.1 ng of the *xKIF13B ORF_DE* mRNA (F). At least 90 cells each were analyzed in three independent experiments. Other abbreviations: Up – up the gradient. Down – down the gradient. L/R – orthogonally to the gradient (to the left/right).

PGCs; this and mechanistic aspects of this process will be in the focus of our future activities.

Supplementary materials related to this article can be found online at doi: 10.1016/j.ydbio.2010.10.016.

Acknowledgments

We thank E. Raz for proving us with EGFP_GRPI_nos and dnPI3K_nos plasmids. This work was supported by funds from the Deutsche Forschungsgemeinschaft to T.P.; K.T. was recipient of a Lichtenberg Stipend in the context of the IMPRS Göttingen.

References

Ara, T., Nakamura, Y., Egawa, T., Sugiyama, T., Abe, K., Kishimoto, T., Matsui, Y., Nagasawa, T., 2003. Impaired colonization of the gonads by primordial germ cells in mice lacking a chemokine, stromal cell-derived factor-1 (SDF-1). Proc. Natl Acad. Sci. USA 100, 5319–5323.

Asaba, N., Hanada, T., Takeuchi, A., Chishti, A.H., 2003. Direct interaction with a kinesin-related motor mediates transport of mammalian discs large tumor suppressor homologue in epithelial cells. J. Biol. Chem. 278, 8395–8400.

Ataman, B., Ashley, J., Gorczyca, D., Gorczyca, M., Mathew, D., Wichmann, C., Sigrist, S.J., Budnik, V., 2006. Nuclear trafficking of *Drosophila* frizzled-2 during synapse development requires the PDZ protein dGRIP. Proc. Natl Acad. Sci. USA 103, 7841–7846.

Berekelya, L.A., Ponomarev, M.B., Luchinskaya, N.N., Belyavsky, A.V., 2003. Xenopus germes encodes a novel germ plasm-associated transcript. Gene Expr. Patterns 3, 521–524.

Blaser, H., Reichman-Fried, M., Castanon, I., Dumstrei, K., Marlow, F.L., Kawakami, K., Solnica-Krezel, L., Heisenberg, C.P., Raz, E., 2006. Migration of zebrafish primordial germ cells: a role for myosin contraction and cytoplasmic flow. Dev. Cell 11, 613–627.

Boldajipour, B., Raz, E., 2007. What is left behind — quality control in germ cell migration. Sci. STKE 383, pe16.

Boldajipour, B., Mahabaleshwar, H., Kardash, E., Reichman-Fried, M., Blaser, H., Minina, S., Wilson, D., Xu, Q., Raz, E., 2008. Control of chemokine-guided cell migration by ligand sequestration. Cell 132, 463–473.

Braithwaite, S.P., Xia, H., Malenka, R.C., 2002. Differential roles for NSF and GRIP/ABP in AMPA receptor cycling. Proc. Natl Acad. Sci. USA 99, 7096–7101.

Charras, G., Paluch, E., 2008. Blebs lead the way: how to migrate without lamellipodia. Nat. Rev. Mol. Cell Biol. 9, 730–736.

Collier, B., Gorgoni, B., Loveridge, C., Cooke, H.J., Gray, N.K., 2005. The DAZL family proteins are PABP-binding proteins that regulate translation in germ cells. EMBO J. 24, 2656–2666.

Doitsidou, M., Reichman-Fried, M., Stebler, J., Koprunner, M., Dorries, J., Meyer, D., Esguerra, C.V., Leung, T., Raz, E., 2002. Guidance of primordial germ cell migration by the chemokine SDF-1. Cell 111, 647–659.

Dong, H., O'Brien, R.J., Fung, E.T., Lanahan, A.A., Worley, P.F., Huganir, R.L., 1997. GRIP: a synaptic PDZ domain-containing protein that interacts with AMPA receptors. Nature 386, 279–284.

Dumstrei, K., Mennecke, R., Raz, E., 2004. Signaling pathways controlling primordial germ cell migration in zebrafish. J. Cell Sci. 117, 4787–4795.

Farini, D., La Sala, G., Tedesco, M., De Felici, M., 2007. Chemoattractant action and molecular signaling pathways of Kit ligand on mouse primordial germ cells. Dev. Biol. 306, 572–583.

Franca-Koh, J., Kamimura, Y., Devreotes, P., 2006. Navigating signaling networks: chemotaxis in *Dictyostelium discoideum*. Curr. Opin. Genet. Dev. 16, 333–338.

Franca-Koh, J., Kamimura, Y., Devreotes, P.N., 2007. Leading-edge research: PtdIns (3,4,5)P3 and directed migration. Nat. Cell Biol. 9, 15–17.

Hara, K., Yonezawa, K., Sakaue, H., Ando, A., Kotani, K., Kitamura, T., Kitamura, Y., Ueda, H., Stephens, L., Jackson, T.R., et al., 1994. 1-Phosphatidylinositol 3-kinase activity is required for insulin-stimulated glucose transport but not for RAS activation in CHO cells. Proc. Natl Acad. Sci. USA 91, 7415–7419.

Heasman, J., Wylie, C.C., 1978. Electron microscopic studies on the structure of motile primordial germ cells of *Xenopus laevis* in vitro. J. Embryol. Exp. Morphol. 46, 119–133.
Heasman, J., Wylie, C.C., 1981. Contact relations and guidance of primordial germ cells on their migratory route in embryos of Xenopus laevis. Proc. R. Soc. Lond. B Biol. Sci. 213, 41–58.
Heasman, J., Hynes, R.O., Swan, A.P., Thomas, V., Wylie, C.C., 1981. Primordial germ cells of Xenopus embryos: the role of fibronectin in their adhesion during migration. Cell 27, 437–447.
Herpin, A., Rohr, S., Riedel, D., Kluever, N., Raz, E., Schartl, M., 2007. Specification of primordial germ cells in medaka (*Oryzias latipes*). BMC Dev. Biol. 7, 3.
Hirokawa, N., Takemura, R., 2005. Molecular motors and mechanisms of directional transport in neurons. Nat. Rev. Neurosci. 6, 201–214.
Hoeller, O., Kay, R.R., 2007. Chemotaxis in the absence of PIP3 gradients. Curr. Biol. 17, 813–817.
Hollemann, T., Panitz, F., Pieler, T., 1999. In situ hybridization techniques with Xenopus embryos. In: Richter, J.D. (Ed.), A Comparative Methods Approach to the Study of Oocytes and Embryos. Oxford University Press Inc., Oxford, pp. 279–290.
Horiguchi, K., Hanada, T., Fukui, Y., Chishti, A.H., 2006. Transport of PIP3 by GAKIN, a kinesin-3 family protein, regulates neuronal cell polarity. J. Cell Biol. 174, 425–436.
Horvay, K., Claussen, M., Katzer, M., Landgrebe, J., Pieler, T., 2006. Xenopus Dead end mRNA is a localized maternal determinant that serves a conserved function in germ cell development. Dev. Biol. 291, 1–11.
Houston, D.W., King, M.L., 2000a. A critical role for Xdazl, a germ plasm-localized RNA, in the differentiation of primordial germ cells in Xenopus. Development 127, 447–456.
Houston, D.W., King, M.L., 2000b. Germ plasm and molecular determinants of germ cell fate. Curr. Top. Dev. Biol. 50, 155–181.
Houston, D.W., Zhang, J., Maines, J.Z., Wasserman, S.A., King, M.L., 1998. A Xenopus DAZ-like gene encodes an RNA component of germ plasm and is a functional homologue of *Drosophila* boule. Development 125, 171–180.
Hudson, C., Woodland, H.R., 1998. Xpat, a gene expressed specifically in germ plasm and primordial germ cells of *Xenopus laevis*. Mech. Dev. 73, 159–168.
Kamimura, M., Kotani, M., Yamagata, K., 1980. The migration of presumptive primordial germ cells through the endodermal cell mass in Xenopus laevis: a light and electron microscopic study. J. Embryol. Exp. Morphol. 59, 1–17.
Kerr, J.B., Dixon, K.E., 1974. An ultrastructural study of germ plasm in spermatogenesis of Xenopus laevis. J. Embryol. Exp. Morphol. 32, 573–592.
Kimura, T., Suzuki, A., Fujita, Y., Yomogida, K., Lomeli, H., Asada, N., Ikeuchi, M., Nagy, A., Mak, T.W., Nakano, T., 2003. Conditional loss of PTEN leads to testicular teratoma and enhances embryonic germ cell production. Development 130, 1691–1700.
King, J.S., Insall, R.H., 2008. Chemotaxis: TorC before you Akt. Curr. Biol. 18, R864–R866.
Kirilenko, P., Weierud, F.K., Zorn, A.M., Woodland, H.R., 2008. The efficiency of Xenopus primordial germ cell migration depends on the germplasm mRNA encoding the PDZ domain protein Grip2. Differentiation 76, 392–403.
Klarlund, J.K., Guilherme, A., Holik, J.J., Virbasius, J.V., Chawla, A., Czech, M.P., 1997. Signaling by phosphoinositide-3, 4, 5-trisphosphate through proteins containing pleckstrin and Sec7 homology domains. Science 275, 1927–1930.
Klisch, T.J., Souopgui, J., Juergens, K., Rust, B., Pieler, T., Henningfeld, K.A., 2006. Mxi1 is essential for neurogenesis in Xenopus and acts by bridging the pan-neural and proneural genes. Dev. Biol. 292, 470–485.
Koebernick, K., Loeber, J., Arthur, P.K., Tarbashevich, K., Pieler, T., 2010. Elr-type proteins protect Xenopus Dead end mRNA from miR-18-mediated clearance in the soma. Proc. Natl Acad. Sci. USA 107, 16148–16153.
Kortholt, A., King, J.S., Keizer-Gunnink, I., Harwood, A.J., Van Haastert, P.J., 2007. Phospholipase C regulation of phosphatidylinositol 3, 4, 5-trisphosphate-mediated chemotaxis. Mol. Biol. Cell 18, 4772–4779.
MacArthur, H., Bubunenko, M., Houston, D.W., King, M.L., 1999. Xcat2 RNA is a translationally sequestered germ plasm component in Xenopus. Mech. Dev. 84, 75–88.
Miki, H., Setou, M., Kaneshiro, K., Hirokawa, N., 2001. All kinesin superfamily protein, KIF, genes in mouse and human. Proc. Natl Acad. Sci. USA 98, 7004–7011.
Molyneaux, K.A., Zinszner, H., Kunwar, P.S., Schaible, K., Stebler, J., Sunshine, M.J., O'Brien, W., Raz, E., Littman, D., Wylie, C., Lehmann, R., 2003. The chemokine SDF1/CXCL12 and its receptor CXCR4 regulate mouse germ cell migration and survival. Development 130, 4279–4286.
Nishiumi, F., Komiya, T., Ikenishi, K., 2005. The mode and molecular mechanisms of the migration of presumptive PGC in the endoderm cell mass of Xenopus embryos. Dev. Growth Differ. 47, 37–48.
Raucher, D., Sheetz, M.P., 2000. Cell spreading and lamellipodial extension rate is regulated by membrane tension. J. Cell Biol. 148, 127–136.
Raucher, D., Stauffer, T., Chen, W., Shen, K., Guo, S., York, J.D., Sheetz, M.P., Meyer, T., 2000. Phosphatidylinositol 4,5-bisphosphate functions as a second messenger that regulates cytoskeleton-plasma membrane adhesion. Cell 100, 221–228.
Schnorrer, F., Kalchhauser, I., Dickson, B.J., 2007. The transmembrane protein Kon-tiki couples to Dgrip to mediate myotube targeting in *Drosophila*. Dev. Cell 12, 751–766.
Stebler, J., Spieler, D., Slanchev, K., Molyneaux, K.A., Richter, U., Cojocaru, V., Tarabykin, V., Wylie, C., Kessel, M., Raz, E., 2004. Primordial germ cell migration in the chick and mouse embryo: the role of the chemokine SDF-1/CXCL12. Dev. Biol. 272, 351–361.
Swan, L.E., Wichmann, C., Prange, U., Schmid, A., Schmidt, M., Schwarz, T., Ponimaskin, E., Madeo, F., Vorbruggen, G., Sigrist, S.J., 2004. A glutamate receptor-interacting protein homolog organizes muscle guidance in *Drosophila*. Genes Dev. 18, 223–237.
Takeuchi, T., Tanigawa, Y., Minamide, R., Ikenishi, K., Komiya, T., 2010. Analysis of SDF-1/CXCR4 signaling in primordial germ cell migration and survival or differentiation in *Xenopus laevis*. Mech. Dev. 127, 146–158.
Tarbashevich, K., Koebernick, K., Pieler, T., 2007. XGRIP2.1 is encoded by a vegetally localizing, maternal mRNA and functions in germ cell development and anteroposterior PGC positioning in *Xenopus laevis*. Dev. Biol. 311, 554–565.
Van Haastert, P.J., Veltman, D.M., 2007. Chemotaxis: navigating by multiple signaling pathways. Sci. STKE pe40.
van Haastert, P.J., Keizer-Gunnink, I., Kortholt, A., 2007. Essential role of PI3-kinase and phospholipase A2 in *Dictyostelium discoideum* chemotaxis. J. Cell Biol. 177, 809–816.
Venkateswarlu, K., Hanada, T., Chishti, A.H., 2005. Centaurin-alpha1 interacts directly with kinesin motor protein KIF13B. J. Cell Sci. 118, 2471–2484.
Waite, K.A., Eng, C., 2002. Protean PTEN: form and function. Am. J. Hum. Genet. 70, 829–844.
Whitington, P.M., Dixon, K.E., 1975. Quantitative studies of germ plasm and germ cells during early embryogenesis of *Xenopus laevis*. J. Embryol. Exp. Morphol. 33, 57–74.
Yoo, S.K., Deng, Q., Cavnar, P.J., Wu, Y.I., Hahn, K.M., Huttenlocher, A., 2010. Differential regulation of protrusion and polarity by PI3K during neutrophil motility in live zebrafish. Dev. Cell 18, 226–236.